

Dipolar Relaxation Dynamics at the Active Site of an ATPase Regulated by Membrane Lateral Pressure

Fischermeier, E.; Pospíšil, P.; Sayed, A.; Hof, M.; Solioz, M.; Fahmy, K.;

Originally published:

December 2016

Angewandte Chemie - International Edition 56(2017)5, 1269-1272

DOI: <https://doi.org/10.1002/anie.201611582>

Perma-Link to Publication Repository of HZDR:

<https://www.hzdr.de/publications/Publ-24433>

Release of the secondary publication
on the basis of the German Copyright Law § 38 Section 4.

Membrane Lateral Pressure Regulates Dipolar Relaxation

Dynamics at the Active Site of an ATPase

Elisabeth Fischermeier^{1,2,+}, Petr Pospíšil³, Ahmed Sayed^{1,2,#}, Martin Hof³, Marc Solioz⁴,
Karim Fahmy^{1,2,*}

¹Helmholtz-Zentrum Dresden-Rossendorf, Institute of Resource Ecology
Bautzner Landstrasse 400, D-01328 Dresden, Germany

²Technische Universität Dresden, Biotechnology Center
Tatzberg 47-49, D-01307 Dresden, Germany

³J. Heyrovský Inst. Physical Chemistry of the A.S.C.R. v.v.i. Prague, Czech Republic

⁴University of Bern, Dept. of Clinical Pharmacology, Murtenstrasse 35, 3008 Bern,
Switzerland

*Corresponding author:

Karim Fahmy

e-mail: k.fahmy@hzdr.de

⁺present address: Nationales Zentrum für Tumorerkrankungen Heidelberg,
Im Neuenheimer Feld 460, D-69120 Heidelberg, Germany

[#]present address: Institute for Experimental Physics I, Universität Leipzig, Linnéstraße 5,
D-04103 Leipzig, Germany

keywords: fluorescence, nanodisc, time-resolved, membrane protein, ion pump

Abstract

The active transport of ions across biological membranes requires their hydration shell to interact with the interior of membrane proteins. However, the influence of the external lipid phase on internal dielectric dynamics is hard to access by experiment. Using the octahelical transmembrane architecture of the copper-transporting P_{1B}-type ATPase from *Legionella pneumophila* as a model structure, we have established the site-specific labeling of internal cysteines with a polarity-sensitive fluorophore. This enabled dipolar relaxation studies in a solubilized form of the protein and in its lipid-embedded state in nanodiscs. Time-dependent fluorescence shifts revealed the site-specific hydration and dipole mobility around the conserved ion-binding motif. The spatial distribution of both features is shaped significantly and independently of each other by membrane lateral pressure.

Integral membrane proteins expose a belt of hydrophobic residues to the interior of the lipid bilayer of the biomembrane in which they are embedded^[1]. The lowest energy state of multi-helical membrane proteins depends on inter-helical contacts, bilayer thickness, and additional lipidic constraints^[2]. Membrane protein function, however, is linked to conformational changes that deviate from the lowest energy state. They are particularly large in P-type ATPases which catalyze ATP-driven ion transport across biological membranes^[3]. The sarcoplasmic P-type Ca²⁺-ATPase SERCA1a provides a mechanistic paradigm for such ion pumps^[4] which switch between two main structural states, E1 and E2, with cytosolic and extracellular accessibility of the ion binding site, respectively. These transitions entail re-adjustments between lipids and the protein^[5]. The functional role of lipid-protein interactions is revealed by the lipid-dependent efficiency of SERCA1a^[6] and is a general characteristic of membrane proteins^[7]. However, molecular specificity is low in comparison to the collective effect of lipids, i.e., thickness and curvature strain, which alter the energetics of membrane protein conformational changes^[8]. P-type ATPases furthermore couple these transitions to ion dehydration and re-hydration during transport. This raises the question whether the hydration and dipole mobility at the non-lipid-exposed internal ion-binding site(s) in a transmembrane helical bundle is yet affected by the collective properties of external lipids.

The experimental determination of the lipid-dependent internal hydration and dipole dynamics of multi-helical membrane proteins has not been attempted, despite their functional importance seen in molecular dynamics (MD) calculations, including P-type ATPases.^[9] Here, we investigated the influence of membrane lateral pressure on the internal hydration of the copper-transporting ATPase LpCopA from *Legionella pneumophila* in nanodiscs (NDs). The latter support native ATPase activity (Fig S3) in a mixed lipid bilayer using the membrane-scaffold protein MSP1E3D1.^[10] Detergents reduce lateral pressure^[8a] rendering the fully solubilized state of a membrane protein a reference state for minimal lateral pressure. As a probe for hydration, we used 6-bromoacetyl-2-dimethylaminonaphthalene (BADAN), a thiol-reactive fluorophore which exhibits changes in time-dependent fluorescence shift (TDFS) in response to changes of hydration in its lipid^[11] or protein environment^[12].

In LpCopA, C382 (the one-letter amino acid code is used throughout) and C384 are part of the conserved CPC motif in transmembrane helix four of P_{1B}-type ATPases and are two key amino acids of the copper binding site. Crystal structures^[9b, 13] suggest their accessibility for chemical modification, rendering LpCopA an ideal model for TDFS studies on intra-membrane protein hydration at minimal structural and mutational perturbation within the octahelical bundle. For specific BADAN-labelling of the CPC motif, native cysteines in

the cytosolic N-terminal domain were changed to serines in the mutant CM-LpCopA (Exp. Section). Its structural integrity after BADAN labeling at C382 and C384 was assessed by circular dichroism (CD). Figure 1A shows that the CD spectrum of labeled CM-LpCopA in NDs is almost identical with the sum of the spectra of empty NDs plus an equimolar amount of BADAN-labeled CM-LpCopA in detergent solution. This confirms a stoichiometry of one CM-LpCopA per ND and agrees with a native secondary structure despite the chemical inactivation of the ion-translocating site. The thermal protein stability was not affected by the label either (Supp. Inf.), in line with tertiary structure conservation. Two additional mutations, C382S or C384S, were introduced into CM-LpCopA, leaving a single cysteine residue in order to bind BADAN, namely to either C382 (CM-B382) or C384 (CM-B384). Dipolar relaxation in the field of the excited state dipole moment lowers the S_1 energy of BADAN, which causes a red shift in fluorescence. The fitted decays and the steady-state emission spectrum were used to reconstruct time-resolved emission spectra (TRES)^[14]. Following the decrease of the peak emission frequency $\nu(t)$ over time, the hydration (micropolarity) and mobility

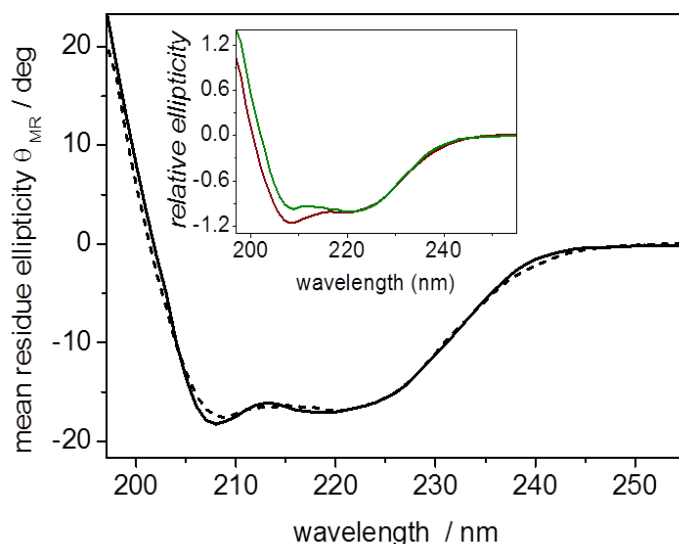


Figure 1: Circular dichroism spectra of the CM-mutant. Solid line: BADAN-labeled CM-LpCopA in NDs. Dashed line: sum of CD spectra of equimolar amounts of the BADAN-labeled CM-LpCopA in detergent solution and empty NDs as shown in the inset in brown and green, respectively.

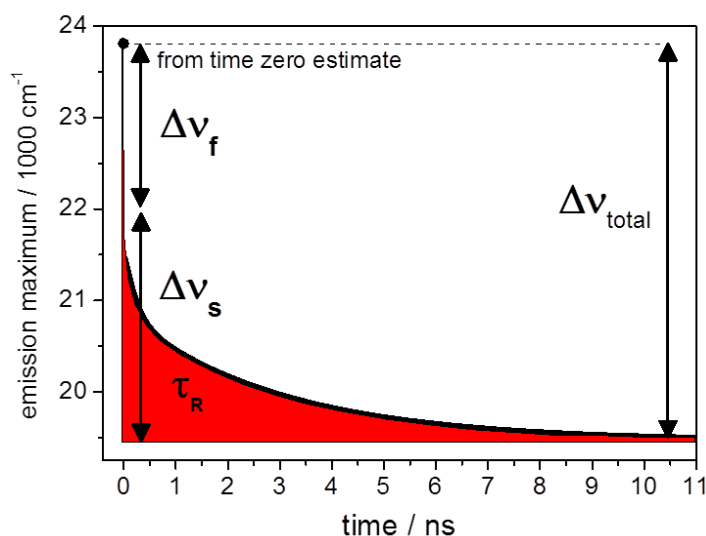


Figure 2: TDFS of BADAN bound to C382. The calculated frequency $\nu(0)$ is displayed as a dot. The total TDFS, $\Delta\nu_{\text{total}}$, covers the shift from $\nu(0)$ to $\nu(\infty)$, accounting for the fast TDFS (less than 30 ps, $\Delta\nu_f$), and the slower experimentally resolved TDFS ($\Delta\nu_s$). The overall TDFS kinetics is derived from the average time constant τ_R .

causes a red shift in fluorescence. The fitted decays and the steady-state emission spectrum were used to reconstruct time-resolved emission spectra (TRES)^[14]. Following the decrease of the peak emission frequency $\nu(t)$ over time, the hydration (micropolarity) and mobility

(microviscosity) in the vicinity of the CPC motif could be assessed. The dipole mobility is proportional to the reciprocal of the average relaxation time (τ_R) in the $\nu(t)$ plot, whereas the total amount of the TDFS, reflects the local polarity and was calculated as: $\Delta\nu_{\text{total}} = \nu(0) - \nu(\infty)$. The frequency $\nu(0)$ of the TRES maximum at $t = 0$ was estimated according to Fee and Maroncelli^[15] taking into account the contribution of relaxation processes faster than the experimental time resolution (30 ps). The frequency $\nu(\infty)$ is defined by the TRES after full dipolar relaxation (for details see Supp. Inf.). The average relaxation time τ_R is proportional to the microviscosity or mobility of the dye microenvironment^[11a] and is derived from the temporal integration of the normalized TDFS.

Figure 2 illustrates time-resolved emission spectra for BADAN bound to C382 in the detergent-solvated state of the protein. Data analysis yielded $\Delta\nu_{\text{total}} = 4300 \text{ cm}^{-1}$ and $\tau_R = 1.14 \text{ ns}$ for the total amount of the TDFS and dipole relaxation time, respectively. The $\nu(0)$ estimate was $23,800 \text{ cm}^{-1}$. The effect of membrane lateral pressure on site-specific hydration was quantified by comparing $\Delta\nu_{\text{total}}$ and τ_R values with those of the same protein preparation after reconstitution into NDs. In the latter, membrane lateral pressure is comparable to that of plasma membranes^[16] which increases inter-helical contacts in the protein and reduces intra-protein dynamics^[17]. The water accessibility around C382 was dramatically restricted in NDs, reducing the total TDFS by 25% ($\Delta\Delta\nu_{\text{total}} = -1100 \text{ cm}^{-1}$, Fig. 3A). Concomitantly, the average relaxation time increased by 20% ($\Delta\tau_R = +0.24 \text{ ns}$), demonstrating reduced local dipole dynamics. A similar correlation of low hydration with low mobility has been demonstrated for active site cavities in soluble proteins^[18]. In contrast to the hydration around C382, the amount of total dipole reorientation in the vicinity of C384 decreased by only 1-2% ($\Delta\Delta\nu_{\text{total}} = -50 \text{ cm}^{-1}$) after reconstitution into NDs, (Fig. 3B). Despite the close α -carbon positions of C382 and C384, dipole relaxation within the octahelical bundle responded differently to membrane lateral pressure. Micropolarity and microviscosity around C382 are tightly controlled by membrane lateral pressure, whereas micropolarity (hydration) is restricted around C384 even in the absence of a membrane. However, the dipole mobility around C384 surprisingly increased with lateral pressure (τ_R shortened by $\sim 0.6 \text{ ns}$) which contrasts the decrease of mobility around C382 in NDs.

Remarkably, the Δv_{total} and τ_R values determined from time-resolved experiments changed to an extent that significantly affected even the static emission spectra (insets in Fig. 3). Although free of kinetic information, these spectra correlate with local dielectric constants of the protein interior (Figs. S4 and S5), providing a widely used scale for intra-membrane protein electrostatics. The apparent relative dielectric constant was close to 5 at both cysteines in NDs but increased mainly around C382 in the solubilized state, where it reached 14 (as compared to 9 at C384). MD calculations suggested C382 to be water accessible in the E2.Pi state, while the corresponding intermediate of SERCA1a does not show water accessibility of the Ca-binding sites^[9b]. The data clearly discriminate the molecular environments of C384 and C382 and reveal opposite responses of the local dipole mobility to lateral pressure.

The dynamic hydration around C382, revealed by TDFS, may originate in the transition between a 'hydrated' and a structurally more constrained 'dehydrated' state of the octahelical bundle. These conformations may be related to intermediate structures that interact with the ion hydration shell or engage in direct ion coordination, respectively. C384 resides in a less mobile environment and is probably constrained by a water-mediated H-bond network.

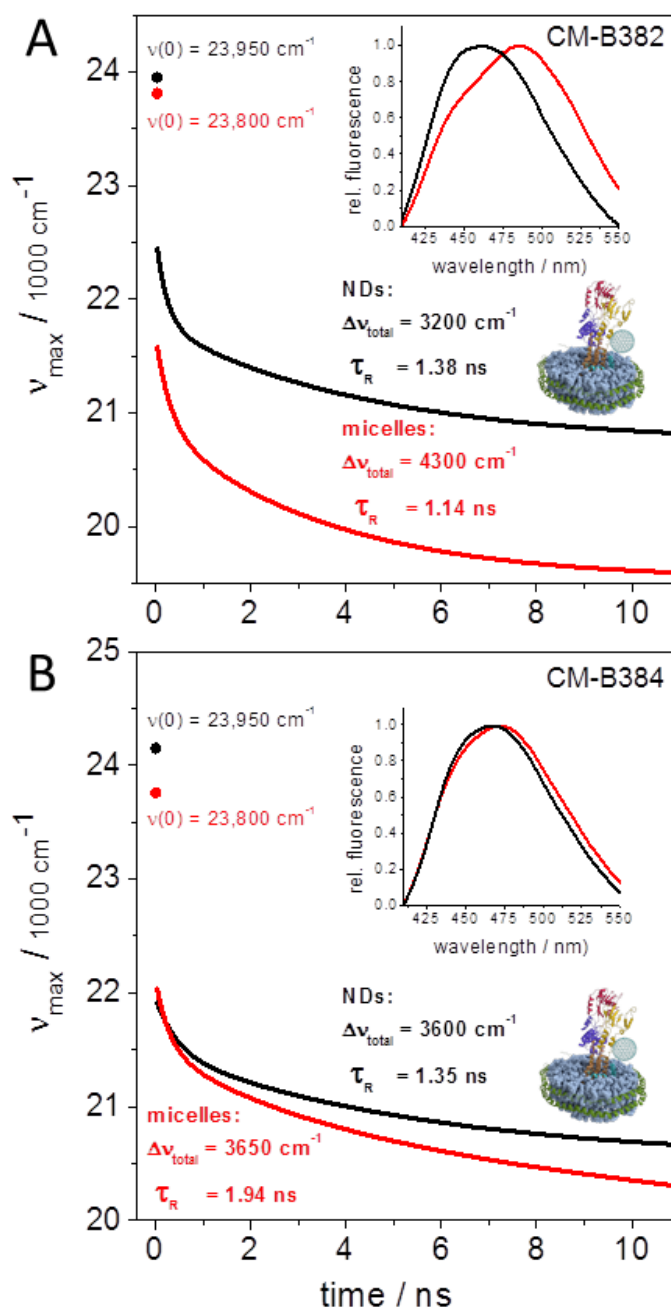
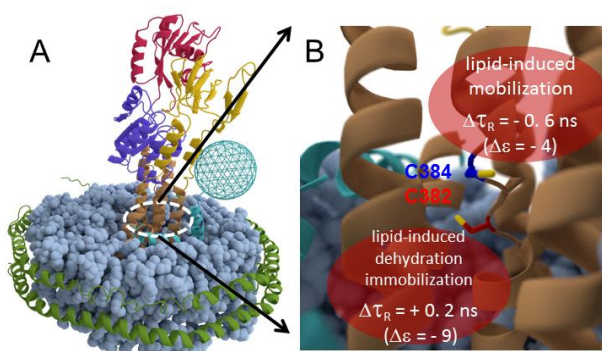


Figure 3: TDFS of BADAN bound to C382 (A) or C384 (B) of the CM-mutant. The $v(0)$ frequencies are displayed as filled circles. Samples were measured in detergent solution (red) and in nanodiscs (black). Insets show the static emission spectra of the two states.

Figure 4: A) Hypothetical topology of LpCopA in NDs. The cytoplasmic phosphorylation, nucleotide-binding and actuator domains are shown in blue, red, and yellow, respectively. Putative location of the N-terminal domain in cyan. B) View of the CPC motif on helix 4. Upon insertion of solubilized LpCopA into NDs, the TDFS local relaxation rate changes by $\Delta\tau_R$, the local dielectric constant by $\Delta\epsilon$. Structure files: pdb 3RFU and 4V6M.



Removal of inter-helical water^[9b] under membrane lateral pressure may thus liberate side chains from the network, leading to the unexpected increase of dipole dynamics in NDs.

Taken together, TDFS resolves distinct patterns of intra-membrane protein hydration and dipole dynamics that are shaped by membrane lateral pressure. The latter may thus act as a restoring force that reverses transient hydration-promoting conformational changes which are presumably required for ion translocation across membranes in general^[19].

Acknowledgements

We thank Jenny Philipp for excellent technical support and Jana Oertel for helpful discussions. Support from Philip Gröger in creating molecular illustrations is gratefully acknowledged. Financial support from GACR (P208/12/G016) and CAS (Praemium Academiae award) is acknowledged.

SUPPORTING INFORMATION

Experimental Section

Accessory Methods

1. Purification and BADAN labeling of recombinant LpCopA
2. Thermal stability of BADAN-labeled LpCopA
3. Reconstitution of LpCopA in nanodiscs
4. ATPase assay
5. Circular dichroism and fluorescence spectroscopy
6. Correlation of static fluorescence spectra with dielectric constants
7. Time zero estimation

Figure S1: Thermal stability of LpCopA

Figure S2: Size-exclusion chromatography of the CM-mutant in nanodiscs

Figure S3: ATPase activity of LpCopA

Figure S4: Analysis of static emission spectra of BADAN-labeled LpCopA

Figure S5: Correlation of emission peak frequencies with apparent dielectric constant.

Table S1: Numerical values of Gaussian band decomposition of static BADAN emission from LpCopA mutants in micelles and NDs

References

- [1] a) F. Cymer, G. von Heijne, S. H. White, *Journal of molecular biology* **2015**, *427*, 999-1022; b) G. von Heijne, *Nature reviews. Molecular cell biology* **2006**, *7*, 909-918.
- [2] F. Cymer, A. Veerappan, D. Schneider, *Bba-Biomembranes* **2012**, *1818*, 963-973.
- [3] a) H.-J. Apell, *Rev. Physiol., Biochem. Pharmacol.* **2003**, *150*, 1-35; b) M. G. Palmgren, P. Nissen, *Annu. Rev. Biophys.* **2011**, *40*, 243-266.
- [4] a) M. Bublitz, M. Musgaard, H. Poulsen, L. Thøgersen, C. Olesen, B. Schiott, J. P. Morth, J. V. Møller, P. Nissen, *J. Biol. Chem.* **2013**, *288*, 10759-10765; b) C. Toyoshima, *Biochim. Biophys. Acta* **2009**, *1793*, 941-946.
- [5] L. Thøgersen, P. Nissen, *Curr. Opin. Struc. Biol.* **2012**, *22*, 491-499.
- [6] A. P. Starling, J. M. East, A. G. Lee, *Biochemistry* **1993**, *32*, 1593-1600.
- [7] A. G. Lee, *Bba-Biomembranes* **2004**, *1666*, 62-87.
- [8] a) J. A. Lundbaek, P. Birn, A. J. Hansen, R. Sogaard, C. Nielsen, J. Girshman, M. J. Bruno, S. E. Tape, J. Egebjerg, D. V. Greathouse, G. L. Mattice, R. E. Koeppe, O. S. Andersen, *J Gen Physiol* **2004**, *123*, 599-621; b) D. Marsh, L. I. Horvath, *Bba-Rev Biomembranes* **1998**, *1376*, 267-296.
- [9] a) F. Guerra, A. N. Bondar, *J Membr Biol* **2014**; b) M. Andersson, D. Mattle, O. Sitsel, T. Klymchuk, A. M. Nielsen, L. B. Møller, S. H. White, P. Nissen, P. Gourdon, *Nat. Struct. Mol. Biol.* **2014**, *21*, 43-48; c) A. N. Bondar, S. H. White, *Biochimica et biophysica acta* **2012**, *1818*, 942-950.
- [10] a) I. G. Denisov, Y. V. Grinkova, A. A. Lazarides, S. G. Sligar, *J. Am. Chem. Soc.* **2004**, *9*, 3477-3487; b) T. H. Bayburt, S. G. Sligar, *FEBS letters* **2010**, *584*, 1721-1727.
- [11] a) P. Jurkiewicz, J. Sykora, A. Olzyska, J. Humpolickova, M. Hof, *Journal of fluorescence* **2005**, *15*, 883-894; b) P. Jurkiewicz, L. Cwiklik, P. Jungwirth, M. Hof, *Biochimie* **2012**, *94*, 26-32; c) R. B. M. Koehorst, S. Laptinok, B. van Oort, A. van Hoek, R. B. Spruijt, I. H. M. van Stokkum, H. van Amerongen, M. a. Hemminga, *Eur. Biophys. J.* **2010**, *39*, 647-656.
- [12] a) M. Amaro, J. Brezovsky, S. Kovacova, L. Maier, R. Chaoupkova, J. Sykora, K. Paruch, J. Damborsky, M. Hof, *Journal of Physical Chemistry B* **2013**, *117*, 7898-7906; b) A. Jesenska, J. Sykora, A. Olzyska, J. Brezovsky, Z. Zdrahal, J. Damborsky, M. Hof, *J Am Chem Soc* **2009**, *131*, 494-501.
- [13] P. Gourdon, X.-Y. Liu, T. Skjørringe, J. P. Morth, L. B. Møller, B. P. Pedersen, P. Nissen, *Nature* **2011**, *475*, 59-64.
- [14] M. L. Horng, J. A. Gardecki, A. Papazyan, M. Maroncelli, *J Phys Chem-Us* **1995**, *99*, 17311-17337.
- [15] R. S. Fee, M. Maroncelli, *Chem Phys* **1994**, *183*, 235-247.
- [16] a) A. W. Shaw, M. a. McLean, S. G. Sligar, *FEBS letters* **2004**, *556*, 260-264; b) D. E. Warschawski, A. a. Arnold, M. Beaugrand, A. Gravel, É. Chartrand, I. Marcotte, *Biochim. Biophys. Acta* **2011**, *1808*, 1957-1974.
- [17] J. Yang, L. Aslimovska, C. Glaubitz, *J. Am. Chem. Soc.* **2011**, *133*, 4874-4881.
- [18] a) A. Jesenská, J. Sýkora, A. Olzyska, J. Brezovský, Z. Zdrahal, J. Damborský, M. Hof, *J. Am. Chem. Soc.* **2009**, *131*, 494-501; b) J. Sykora, J. Brezovsky, T. Koudelakova, M. Lahoda, A. Fortova, T. Chernovets, R. Chaloupkova, V. Stepankova, Z. Prokop, I. K. Smatanova, M. Hof, J. Damborsky, *Nat. Chem. Biol.* **2014**, *10*, 428-430.
- [19] a) Y. A. Mahmmoud, W. Kopec, H. Khandelia, *J. Biol. Chem.* **2015**, *290*, 3720-3731; b) J. Li, S. A. Shaikh, G. Enkavi, P. C. Wen, Z. Huang, E. Tajkhorshid, *Proc. Natl. Acad. Sci. U. S. A.* **2013**, *110*, 7696-7701.
- [20] T. K. Ritchie, Y. V. Grinkova, T. H. Bayburt, I. G. Denisov, J. K. Zolnerciks, W. M. Atkins, S. G. Sligar, *Methods Enzymol.* **2009**, *464*, 211-231.